

for the specification of the region (8, 11, 12). We examined the expression of these genes in *Lhx5* mutant embryos. At E12.5, all three of these genes were expressed in the hippocampal anlagen in both wild-type (Fig. 4, A through C) and mutant (Fig. 4, F through H) embryos, which indicates that the hippocampal precursor cells were specified after disruption of *Lhx5*. In the mutant embryos, the domains of *Lhx2*, *Emx2*, and *Otx1* expression expanded ventrally into the region of the telencephalic choroid plexus, and morphogenesis of the choroid plexus was impaired. Signaling molecules of the *Wnt* and *Bmp* families have been implicated in patterning the medial telencephalic wall to form the hippocampal anlagen and the choroid plexus, because these molecules are expressed at the border between these two morphologically distinctive structures (13, 14) (Fig. 4, D and E). In support of this idea, expression of *Wnt5a* (Fig. 4I), *Bmp4*, and *Bmp7* (Fig. 4J) was diminished in this specific region in *Lhx5* null mutant embryos.

Previous experiments have shown that other members of the LIM homeobox gene family play crucial roles in the differentiation of distinct cell types in various organisms (15–18). In mice, for example, *Islet1* is essential for the differentiation of motor neurons in the spinal cord (15), and *Lhx3* is required for the differentiation of the pituitary cell lineages (16). More recently, it has been observed that *Lhx3* and *Lhx4* together control the axon projection of subtypes of motor neurons as well as their exact soma position in the developing spinal cord (17). Our data suggest that *Lhx5* may play an analogous role in the developing forebrain.

Defects in hippocampal development have been observed in mice carrying null mutations in a variety of genes. Functional ablation of the homeobox gene *Emx2* (11) or *Lhx2* (8) leads to an early arrest of hippocampal development as precursor cells fail to be specified or to proliferate. Mutations in *Reeler* (5), *Mdab1* (19), *Cdk5* (20), *P35* (21), and *Pafah1b1* (22) impair neuronal migration, resulting in a disorganization of cells in Ammon's horn and the dentate gyrus. Our results show that *Lhx5* is required for differentiation of the various types of hippocampal neurons. Together, these studies reveal an intricate genetic program underlying the assembly of complex hippocampal structures.

Expression of *Lhx5* after E13.5 in the Cajal-Retzius cells raises the possibility that the impairment in hippocampal morphogenesis observed in *Lhx5* mutant embryos could result from a lack of function of those cells. The gene *Reeler* is expressed in these cells (5), in keeping with the possibility that this gene might be a downstream target of *Lhx5*. However, the defects in morphogenesis as well as in neuronal differentiation of Ammon's horn and the dentate gyrus seen in the *Lhx5* mutant embryos are

more severe than those of *Reeler* (5), *Mdab1* (19), *Cdk5* (20), *P35* (21), and *Pafah1b1* (22) mutants, which suggests that *Lhx5* may control a different pathway. The *Lhx5* knockout mice provide a model to further understand the molecular and cellular mechanisms underlying the formation of Ammon's horn and the dentate gyrus and their functions in cognition, learning, and memory.

References and Notes

1. V. S. Caviness Jr., *J. Comp. Neurol.* **151**, 113 (1973); B. B. Stanfield and W. M. Cowan, *ibid.* **185**, 423 (1979); S. A. Bayer, *ibid.* **190**, 115 (1980).
2. H. Z. Sheng et al., *Dev. Dyn.* **208**, 266 (1997).
3. R. Toyama et al., *Dev. Biol.* **170**, 583 (1995).
4. E. Soriano, J. A. Del Rio, A. Martinez, H. Super, *J. Comp. Neurol.* **342**, 571 (1994).
5. G. D'Arcangelo et al., *Nature* **374**, 719 (1995); K. Nakajima, K. Mikoshiba, T. Miyata, C. Kudo, M. Ogawa, *Proc. Natl. Acad. Sci. U.S.A.* **94**, 8196 (1997).
6. J. A. Del Rio et al., *Nature* **385**, 70 (1997).
7. S. Bertuzzi et al., *Genomics* **36**, 234 (1996).
8. F. D. Porter et al., *Development* **124**, 2935 (1997).
9. Neuron-specific class III β -tubulin was detected by Tuj-1 antibody (BabCo, 1:5000).
10. TUNEL staining was performed on paraffin sections with a Neuro TACS II kit (Trevigen).
11. M. Pellegrini, A. Mansouri, A. Simeone, E. Boncinelli, P. Gruss, *Development* **122**, 3893 (1996); M. Yoshida et al., *ibid.* **124**, 101 (1997).
12. A. Simeone et al., *EMBO J.* **12**, 2735 (1993).
13. E. A. Grove, S. Tole, J. Limon, L. Yip, C. W. Ragsdale, *Development* **125**, 2315 (1998).
14. Y. Furuta, D. W. Piston, B. L. M. Hogan, *ibid.* **124**, 2203 (1997).
15. S. L. Pfaff, M. Mendelsohn, C. L. Stewart, T. Edlund, T. M. Jessell, *Cell* **84**, 309 (1996).

16. H. Z. Sheng et al., *Science* **272**, 1004 (1996).
17. K. Sharma et al., *Cell* **95**, 817 (1998).
18. I. B. Dawid, J. J. Breen, R. Toyama, *Trends Genet.* **14**, 156 (1998); J. C. Way and M. Chalfie, *Cell* **54**, 5 (1988); G. Freyd, S. K. Kim, H. R. Horvitz, *Nature* **344**, 876 (1990); O. Hobert et al., *Neuron* **19**, 345 (1997); O. Hobert, T. D'Alberti, Y. Liu, G. Ruvkun, *J. Neurosci.* **18**, 2084 (1998); C. Bourgouin, S. E. Lundgren, J. B. Thomas, *Neuron* **9**, 549 (1992).
19. M. Sheldon et al., *Nature* **389**, 730 (1997); B. W. Howell, R. Hawkes, P. Soriano, J. A. Cooper, *ibid.*, p. 733.
20. T. Ohshima et al., *Proc. Natl. Acad. Sci. U.S.A.* **93**, 11173 (1996).
21. T. Chae et al., *Neuron* **18**, 29 (1997).
22. S. Hirotsune et al., *Nature Genet.* **19**, 333 (1998).
23. G. W. Robinson, S. Wray, K. A. Mahon, *New Biol.* **3**, 1183 (1991).
24. A. Simeone et al., *EMBO J.* **11**, 2541 (1992).
25. Y. Xu et al., *Proc. Natl. Acad. Sci. U.S.A.* **90**, 227 (1993).
26. B. J. Gavin, J. A. McMahon, A. P. McMahon, *Genes Dev.* **4**, 2319 (1990).
27. Embryos were fixed with 4% paraformaldehyde by immersion (E10.5 to E12.5) or transcardial perfusion (E15.5 to E18.5) and embedded in paraffin. Sections (5 μ m) were cut and processed for in situ hybridization by published procedures (23). The probes used for in situ hybridization were specific for *Emx2* (24), *Lhx2* (25), *Lhx5* (2), *Otx1* (12), *Wnt5a* (26), *Bmp4*, and *Bmp7* (14).
28. A. Nagy, J. Rossant, R. Nagy, W. Abramow-Newerly, J. C. Roder, *Proc. Natl. Acad. Sci. U.S.A.* **90**, 8424 (1993).
29. We thank E. Boncinelli for *Otx1* and *Emx2* probes, B. L. Hogan for *Bmp4* and *Bmp7* probes, F. D. Porter for the *Lhx2* probe, A. McMahon for the *Wnt5a* probe, R. Wenthold for the antiserum to GluR1, and X. Jian, K. Pfeifer, S. Shtrom, A. Tomac, and M. Fiorenza for comments on the manuscript.

3 December 1998; accepted 15 April 1999

Separate Signals for Target Selection and Movement Specification in the Superior Colliculus

Gregory D. Horwitz and William T. Newsome*

At any given instant, multiple potential targets for saccades are present in the visual world, implying that a "selection process" within the brain determines the target of the next eye movement. Some superior colliculus (SC) neurons begin discharging seconds before saccade initiation, suggesting involvement in target selection or, alternatively, in postselectional saccade preparation. SC neurons were recorded in monkeys who selected saccade targets on the basis of motion direction in a visual display. Some neurons carried a direction-selective visual signal, consistent with a role in target selection in this task, whereas other SC neurons appeared to be more involved in postselection specification of saccade parameters.

The primate SC plays a major role in the generation of saccades. Many neurons in the intermediate and deep layers of the SC fire a

brief burst of action potentials starting approximately 20 ms preceding saccades of a particular range of directions and amplitudes; the region defined by the end points of such saccades comprises the "movement field" of an SC neuron. For each neuron, the location of the movement field in space varies systematically with the location of the neuron in the SC (1–4). Many SC neurons exhibit a "pre-

Howard Hughes Medical Institute and Department of Neurobiology, Stanford University School of Medicine, Stanford, CA 94305, USA.

*To whom correspondence should be addressed. E-mail: bill@monkeybiz.stanford.edu

REPORTS

lude” of activity related to the metrics of an impending saccade up to several seconds before the saccade is actually executed, implicating the SC in higher-level aspects of saccade planning (5–7). It is not known, however, whether these signals play a role in target selection, or simply reflect motor plans formed in response to selection processes elsewhere in the brain.

We investigated the role of the SC in target selection by recording prelude cells in monkeys (*Macaca mulatta*) trained to select one of two possible saccade targets contingent upon the direction of motion in a visual stimulus presented on a cathode ray tube monitor (Fig. 1) (8). For each SC neuron studied, the geometry of the display was arranged so that one of the targets (T1) lay inside the cell’s movement field, while the other (T2) lay outside the movement field.

We recorded the activity of 96 intermediate and deep-layer SC neurons whose prelude activity was greater preceding T1 choices than T2 choices, permitting an experimenter to predict the monkey’s decision several seconds before the saccade (9). Figure 2 illustrates the responses of a predictive SC neuron; three aspects of these responses are consistent with a role in target selection. First, predictive activity developed during the stimulus presentation interval while the monkey was formulating its judgment of motion direction. Second, predictive activity developed later and more gradually for low coherence trials than for high coherence trials, consistent with the longer psychophysical integration times required to discriminate weak motion signals (10, 11). Third, this cell lacked a saccade-locked burst, suggesting that it plays only a minor role in saccade execution.

Neurons involved in target selection in our task may receive relatively direct sensory inputs concerning the direction of motion in the visual stimulus; the logic of the task dictates that such neurons should be excited selectively by motion flowing toward their movement fields. To test for the presence of such inputs in the SC, we looked for directional visual responses in blocks of trials when the monkey was rewarded for passive fixation (12). Random dot stimuli were presented within a circular aperture surrounding the center of gaze; the direction of coherent motion was either toward or away from the movement field of the SC neuron. Of the 96 choice-predicting SC neurons, 44 yielded directional responses: activity was significantly stronger when motion flowed toward the movement field than away from it (Mann-Whitney U-test: $P < 0.05$). No cell was significantly more active when motion flowed away from the movement field.

A possible criticism of these experiments is that, by force of habit, our monkeys may have planned saccadic eye movements co-

vertly upon viewing the moving random dots even though they were not required to execute such movements. To control for this possibility, we measured visual direction tuning curves for 22 neurons when the monkey was required to plan saccades to a location outside of the movement field of the cell (Fig. 3A). In this condition, a single saccade target appeared early in the trial, and visual direction tuning curves were measured by presenting stimuli during the overlap period while the monkey awaited a “go” signal before executing the saccade (13). Because the monkey is able to plan the saccade from the beginning of the trial, it is unlikely that random dot motion during the overlap period would elicit covert saccade planning to a different, unrewarded location.

Direction tuning curves measured during the saccade task (14) did not differ from those measured during passive fixation trials in terms of preferred direction (Wilcoxon signed rank test, $P > 0.5$), tuning width ($0.1 > P > 0.05$), or amplitude of response ($P > 0.5$). The preferred direction of the cell to visual motion measured in the saccade task (arrow, Fig. 3B) corresponded well with the direction of the saccades elicited by electrical stimulation at the same site (arrow, Fig. 3A). This correlation held up well across all 22

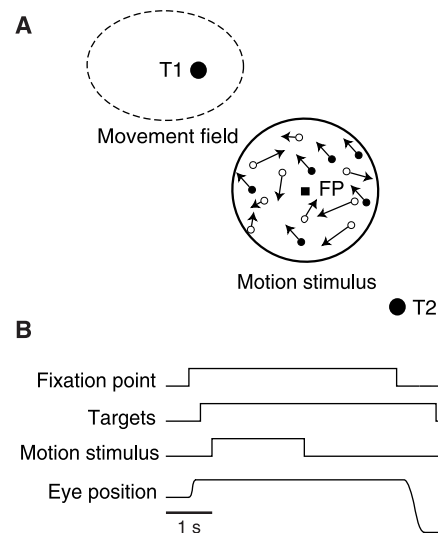


Fig. 1. (A) Geometry of the visual display and (B) the timing of events in the direction discrimination task. The motion stimulus appeared within a circular aperture subtending 7° of visual angle and was usually presented at the center of gaze. Saccade targets were illuminated 300 ms after the monkey acquired the fixation point. Then, 500 to 900 ms later, a 2000-ms motion stimulus was presented, followed by an enforced delay period lasting 1000 to 1500 ms. Disappearance of the fixation point cued the monkey to make a saccade. Fixation breaks aborted trials. Eye position was continuously monitored by the scleral search coil technique (28). Horizontal and vertical eye position was sampled at a rate of 1 kHz and stored at a rate of 250 Hz for off-line analysis.

neurons tested (Fig. 3C, circular-circular rank correlation coefficient: $r = 0.77$, $P < 0.0001$).

These direction-selective responses have not been documented previously in primate SC. An intriguing possibility is that, over the course of training, pathways between visual cortex and SC neurons involved with target selection are modified so as to mediate this learned association (15). Indeed, recordings in a monkey that had not been trained to associate particular directions of motion with particular saccade vectors revealed substantially fewer direction-selective SC neurons (5/35 versus 44/96: z-test $P < 0.001$) (16).

The two groups of prelude neurons may represent different neural processing levels, one involved in target selection and the other in the specification of saccade parameters. We analyzed the time course of predictive activity in each group of neurons (Fig. 4) (17, 18). In the direction-selective cells, predictive activity developed with a short latency and a rapid time course, suggestive of an early role in saccade planning. The magnitude of the

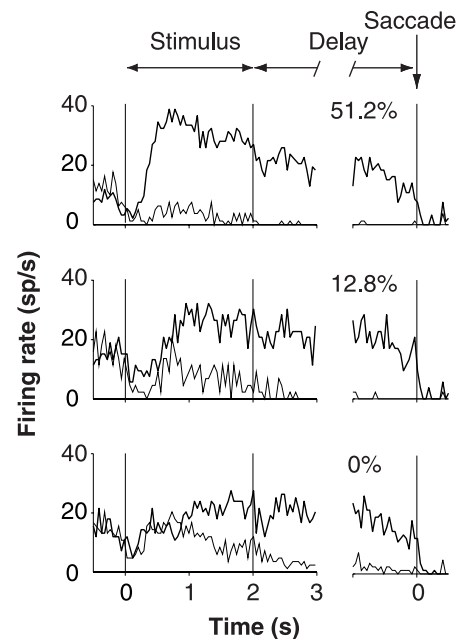


Fig. 2. Peristimulus and perisaccade time histograms for the discharge of a single superior colliculus neuron during direction discrimination at three different stimulus coherences. Data from correct trials only are displayed (except at 0% coherence for which correctness is arbitrary). Thick and thin curves illustrate the mean response preceding T1 choices and T2 choices, respectively. The left half-panel of each plot is aligned on motion stimulus presentation. The right half-panels show data from the same trials aligned on saccade initiation. The gap between the two half-panels reflects the timing variability between stimulus offset and saccade initiation. Vertical lines indicate the time of stimulus onset, stimulus offset, and saccade initiation, and the unit sp/s is spikes per second.

predictive activity during the stimulus presentation was strongly modulated by the motion coherence (Spearman's $r = 0.94$; $P < 0.025$). Thus, the activity of these cells reflects not only the animal's decision, but also the strength of the signal upon which the decision is based (19, 20). Finally, these cells exhibited predictive activity up to 500 ms

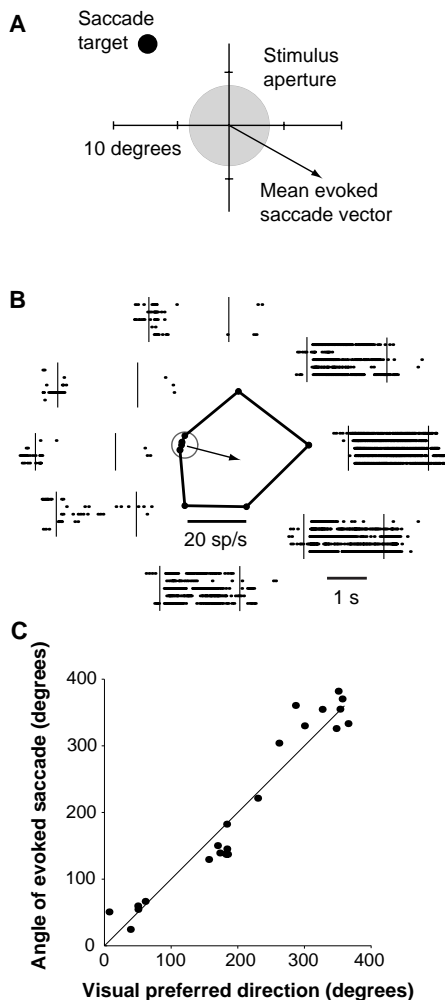


Fig. 3. (A) Spatial design of a typical direction tuning measurement. Fixation was at the intersection of the axes. The gray disk shows the spatial extent of the stimulus aperture. The arrow depicts the average end point of 15 saccades elicited by electrical stimulation at the recording site; this provides an estimate of the movement field location of nearby cells. On each trial the monkey was required to make a saccade to a single target located far from the movement field of the cells at the recording site. (B) Averaged and raw responses of an SC neuron to eight directions of motion. Rasters illustrate raw responses to each of the eight directions. The polar plot depicts the average response as a function of motion direction. Background activity is represented by the circle at the origin of the polar plot. Vertical bars in the rasters delimit the 2000-ms stimulus presentation. The arrow indicates the estimated preferred direction of the cell. (C) Scatterplot of preferred direction against angle of electrically elicited saccades.

before the presentation of the 0% coherence visual stimulus (Fig. 4A, arrow; permutation tests: $P < 0.01$ at each time point) (21). This activity may reflect intrinsic bias states which can influence the animal's decision in the absence of strong sensory signals (22).

Non-direction selective cells differed from direction-selective cells in each of these respects. Predictive activity developed with a longer latency and slower time course (permutation tests: $P < 0.025$ and $P < 0.01$, respectively) (23), and was not modulated by stimulus coherence (Spearman's $r = 0.26$; $P > 0.25$). In addition, these cells did not exhibit predictive activity in the interval preceding the stimulus presentation (permutation tests: $P > 0.1$ at each time point).

Analysis of perisaccadic neural activity suggests that the non-direction selective cells are more closely involved with saccade execution. For saccades directed toward the target in the movement field, perisaccadic firing rates (recorded during an interval from 50 ms before until 25 ms after the saccade initiation) were almost three times greater in non-direction selective cells than in direction-selective cells (116 spikes/s versus 40 spikes/s; Mann-Whitney U-test: $P < 0.0001$).

The direction-selective cells we describe appear appropriate for implementing the association between motion stimuli and saccade vectors that is necessary for correct perfor-

mance on our task. Mays and Sparks described a high-level class of SC neurons ("quasi-visual" cells) that appear to represent potential targets for saccadic eye movements, but are not linked obligatorily to execution of a saccade (5). Similarly, Basso and Wurtz described SC neurons whose activity reflects the probability that a saccade will be made into their movement fields (24). Either or both of these populations may overlap with our direction-selective neurons.

Our data suggest that at least two levels of processing related to saccade planning are present within the SC. Some cells possess a constellation of properties indicative of a high-level role in decision formation and target selection, while other cells are more directly linked to saccade execution. These two profiles appear to lie at opposite ends of a continuum rather than representing two distinct, nonoverlapping populations of cells. Previous studies have identified neurons in the lateral intraparietal area (LIP) and prefrontal cortex that carry signals appropriate for mediating decision formation, target selection, or saccade planning (15, 19, 20, 25–27). It will be important to determine how these formal processes are distributed among the several brain areas and how neuronal populations in these areas interact to accomplish these tasks.

References and Notes

1. P. H. Schiller and F. Koerner, *J. Neurophysiol.* **34**, 915 (1971).
2. R. H. Wurtz and M. E. Goldberg, *Science* **171**, 82 (1971).
3. ———, *J. Neurophysiol.* **35**, 575 (1972).
4. D. L. Sparks, *Brain Res.* **156**, 1 (1978).
5. L. E. Mays and D. L. Sparks, *J. Neurophysiol.* **43**, 207 (1980).
6. P. W. Glimcher and D. L. Sparks, *Nature* **355**, 542 (1992).
7. D. P. Munoz and R. H. Wurtz, *J. Neurophysiol.* **73**, 2313 (1995).
8. Three monkeys were trained to discriminate opposite directions of motion in a stochastic visual display centered on the fovea. The stimulus was a circular field of randomly positioned dots, a proportion of which translated coherently in a specified direction whereas the remainder were replotted at random locations on successive video frames. On each trial, the monkey reported the direction of motion of the coherent dots by making a saccade to one of two targets presented at either end of the motion axis. The difficulty of the task was pseudo-randomly varied from trial to trial by changing the proportion of coherently moving dots. The monkey received liquid rewards for choosing the target in the direction of coherent motion.
9. While the monkeys performed the task, we qualitatively assessed prelude activity in 704 intermediate and deep-layer SC neurons. Roughly 25% of the cells exhibited target-specific prelude activity several seconds before saccade execution. We obtained quantitative data sets from 127 neurons. For each of these cells, we counted spikes during the presentation of the motion stimulus and the first second of the delay period. The counts were normalized within each stimulus coherence and compiled into two distributions according to the monkey's choice in the discrimination task (T1 or T2). For each cell, the difference between these two distributions was evaluated by a Mann-Whitney U-test with a criterion level of $P < 0.01$. By this criterion, 103 of 127 cells exhibited predictive activity. Seven of these cells were elimi-

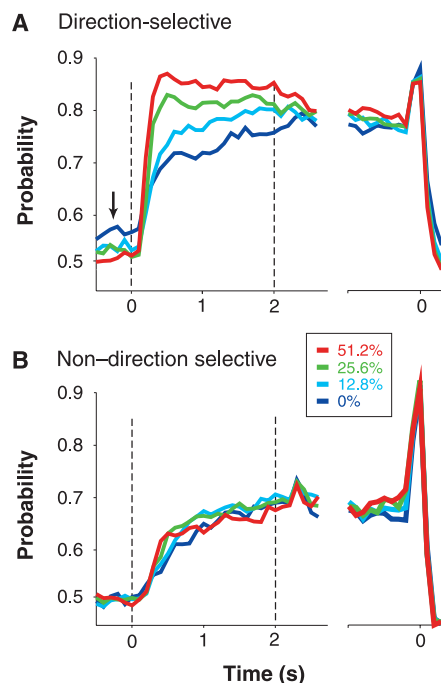


Fig. 4. Ideal observer analysis on pooled data from (A) direction-selective neurons ($n = 44$) and (B) non-direction selective neurons ($n = 52$). Trials are aligned on the presentation of the motion stimulus (times 0 through 2 in the left half-panels) and saccade initiation (time 0 in the right half-panels). Curve color corresponds to motion coherence.

nated from further analysis because they were significantly more active preceding saccades to T2 than to T1. Thus, our final database consisted of 96 choice-predicting SC neurons.

10. K. H. Britten, M. N. Shadlen, W. T. Newsome, J. A. Movshon, *J. Neurosci.* **12**, 4745 (1992).
11. J. D. Roitman and M. N. Shadlen, *Soc. Neurosci. Abstr.* **24**, 262 (1998).
12. For each cell isolated, we presented 6 to 15 repetitions of a 51.2% coherence stimulus of 1- to 2-s duration, moving either toward or away from the movement field.
13. In saccade trials, a single target was illuminated contralateral to the cell's movement field 300 ms after the monkey fixated. This event indicated to the monkey that a saccade to the target (within 500 ms of fixation point disappearance) would be required in order to obtain a reward. Saccade and passive fixation trials were randomly interleaved.
14. Direction tuning curves were parameterized by least-squares fits of Gaussian functions to mean firing rates according to the following equation:

$$\text{firing_rate} = \text{baseline} + \text{amplitude} \times \exp[-(\text{motion_dir} - \text{pref_dir})^2 / (2 \times \text{width}^2)]$$
15. N. P. Bichot, J. D. Schall, K. G. Thompson, *Nature* **381**, 697 (1996).
16. This monkey was trained to perform a direction discrimination task in which the mapping between the direction of visual motion and the operant saccade vector varied substantially from trial to trial. Direction selectivity was measured during a passive fixation task, as it was for the other monkeys in this study. Only 5 of 35 intermediate-layer neurons exhibited significant direction selectivity (Mann-Whitney U-test: $P < 0.05$). Data from this animal will be described fully elsewhere.
17. We performed this analysis separately for each motion strength using only correctly answered trials. Time was quantized in nonoverlapping 100-ms bins spanning the trial. We calculated normalized activity for each cell by counting the number of spikes in each time bin and dividing by the maximum mean spike count (mean across trials, maximum across motion strengths and time bins). Normalized spike counts were first pooled across cells and then segregated with respect to the monkey's psychophysical decision. For each time bin, we calculated an ROC (receiver operating characteristic) curve from the two distributions of spike counts and integrated its area. This metric can be interpreted as the probability with which an ideal observer could predict the monkey's choice on the basis of the normalized spike count in that time bin.
18. D. M. Green and J. A. Swets, *Signal Detection Theory and Psychophysics* (Wiley, New York, 1966).
19. M. N. Shadlen and J. N. Kim, *Nature Neurosci.* **2**, 176 (1998).
20. M. Shadlen and W. Newsome, *Proc. Natl. Acad. Sci. U.S.A.* **93**, 628 (1996).
21. For each of the five 100-ms-long epochs preceding the onset of the visual stimulus, we assigned spike counts from T1 choice trials and T2 choice trials randomly to two distributions. We then calculated the ROC curve for the two distributions and integrated its area. This procedure was repeated 5000 times to estimate the distribution of ROC areas that would be expected by chance. The cited P value indicates the proportion of the 5000 iterations in which the ROC value computed from the randomized data equaled or exceeded the ROC value computed from the experimental (nonrandomized) data.
22. We suggest that the monkey enters some trials favoring one target over the other, and that this bias is reflected in small firing rate differences before onset of the visual stimulus. When the motion coherence is high, the direction of stimulus motion largely determines the monkey's choices, overriding the weak bias that exists entering the trial. Because the direction of stimulus motion is chosen randomly, trials in which the monkey is biased toward T1 or T2 have an equal probability of resulting in a T1 or T2 decision, and little or no differential activity is apparent when the trials are subsequently sorted and analyzed according to decision outcome. At 0% coherence, however, the

monkey tends to choose in the direction of the bias because there is no directional signal to override the bias. Thus, the small differences in neural activity associated with the bias (before stimulus onset) become associated with the decision and are apparent when the trials are sorted and analyzed according to decision outcome.

23. All coherences were averaged together for these analyses. Latency was defined as the time from stimulus onset until predictive activity exceeded the baseline level by three standard deviations. Time was quantized in 10-ms bins for this analysis because the difference in latency between the two groups was only 30 ms. For the time course analysis we calculated the time to reach half of the maximum predictive activity obtained during the stimulus presentation. This time differed between the two groups by 300 ms. Distributions of both statistics under the null hypothesis were generated by randomly reassigning the cells to two groups 2000 times, calculating the value of the statistic for both groups, and recording the difference. The cited P value is the proportion of differences greater than or equal to the actual difference obtained from the nonrandomized data.

24. M. A. Basso and R. H. Wurtz, *J. Neurosci.* **18**, 7519 (1998).
25. J. W. Gnadt and R. A. Andersen, *Exp. Brain Res.* **70**, 216 (1988).
26. J. Schall and D. Hanes, *Nature* **366**, 467 (1993).
27. P. Mazzoni, R. Bracewell, S. Barash, R. Andersen, *J. Neurophysiol.* **76**, 1439 (1996).
28. D. A. Robinson, *IEEE Trans. Biomed. Eng.* **10**, 137 (1963).
29. We thank C. Barberini, G. DeAngelis, J. Liu, J. Nichols, and M. Shadlen for critical feedback and comments on the manuscript. All experimental procedures and care of the animals were carried out in compliance with guidelines established by NIH and approved by the Institutional Animal Care and Use Committee of Stanford University. Supported by the National Eye Institute (grant 05603) and by the Human Frontiers Science Research Program. G.D.H. was supported by a predoctoral fellowship from the Office of Naval Research and by training grant 5T32NH17047-17 from NIH. W.T.N. is an Investigator with the Howard Hughes Medical Institute.

9 November 1998; accepted 8 April 1999

Interaction of RAFT1 with Gephyrin Required for Rapamycin-Sensitive Signaling

David M. Sabatini,^{1*} Roxanne K. Barrow,¹ Seth Blackshaw,¹
 Patrick E. Burnett,¹ Michael M. Lai,¹ Michael E. Field,¹
 Ben A. Bahr,² Joachim Kirsch,³ Heinrich Betz,³
 Solomon H. Snyder^{1†}

RAFT1 (rapamycin and FKBP12 target 1; also called FRAP or mTOR) is a member of the ATM (ataxia telangiectasia mutated)-related family of proteins and functions as the *in vivo* mediator of the effects of the immunosuppressant rapamycin and as an important regulator of messenger RNA translation. In mammalian cells RAFT1 interacted with gephyrin, a widely expressed protein necessary for the clustering of glycine receptors at the cell membrane of neurons. RAFT1 mutants that could not associate with gephyrin failed to signal to downstream molecules, including the p70 ribosomal S6 kinase and the eIF-4E binding protein, 4E-BP1. The interaction with gephyrin ascribes a function to the large amino-terminal region of an ATM-related protein and reveals a role in signal transduction for the clustering protein gephyrin.

Proteins of the ATM family participate in cell cycle progression by linking signals from growth factor receptors and internal checkpoints to the cell cycle machinery. These cell cycle regulators are members of the kinase superfamily and include the gene product of the ataxia telangiectasia locus (*ATM*), the

catalytic subunit of the DNA-activated protein kinase (DNA-PKcs), RAFT1 or FRAP, and the products of the yeast genes *TOR1*, *TOR2*, and *TEL1* (1).

RAFT1 and its yeast homologs, the TOR proteins, are the *in vivo* targets for the complex of rapamycin with its intracellular receptor, FKBP12. Rapamycin is a potent immunosuppressant that prevents progression through the G₁ phase of the cell cycle in various cell types, including T lymphocytes and budding yeast (2). The effects of rapamycin point to a role for RAFT1 and the TORs in cell cycle regulation, and increasing evidence indicates that they participate in mitogen-stimulated signaling pathways that control mRNA translation. In mammalian cells RAFT1 controls the rapamycin-sensitive phosphorylation of at least two transla-

¹The Johns Hopkins University School of Medicine, Department of Neuroscience, 725 North Wolfe Street, Baltimore, MD 21205, USA. ²Department of Pharmaceutical Sciences, University of Connecticut, Storrs, CT 06269, USA. ³Department of Neurochemistry, Max Planck Institute for Brain Research, Deutscherordenstrasse 46, 60528 Frankfurt/Main, Germany.

*Present address: Whitehead Institute for Biomedical Research, 9 Cambridge Center, Cambridge, MA 02142, USA.

†To whom correspondence should be addressed. E-mail: ssnyder@jhmi.edu